

Investigation of Production Parameters, Mechanical Properties and Microstructures of 5005 Aluminum Alloys Produced by St/Cu Shell Pair in TRC

Furkan Berkay Tamer^{*1}, Serdar Aslan², Onur Birbaşar³

^{*1} Faculty of Engineering, Karadeniz Technical University, Trabzon, TÜRKİYE

² Faculty of Engineering, Sakarya University, Sakarya, TÜRKİYE

³ ASAŞ Alüminyum Sanayi ve Ticaret A.Ş., Sakarya, TÜRKİYE

(Received: 02.04.2024, Accepted: 25.04.2024, Published Online: 26.04.2024)

Keywords

Twin Roll Casting,
TRC,
Copper shell,
Recrystallization,
Aluminum

ABSTRACT

This study was carried out on the rollers where solidification occurs in the twin-roll casting method being one of the flat product manufacturing methods. The rollers where solidification occurs consist of two components, the core and the shell. These are cooled by water circulation. In industry, alloy forged steel is commonly used as the shell material. It is known that the copper has a higher thermal conductivity coefficient than that of steel. That's why, copper shell material can be used industrially instead of steel due to its advantages such as rapid solidification and increasing productivity. In this study, instead of alloy steel/steel shell, steel/copper shell pair was used and the effects of this shell pair on the production parameters, microstructural and mechanical properties of 5005 aluminum alloy were examined. Consequently, 40-60% of productivity has been achieved. Thanks to the Cu shell, partial dynamic recrystallization occurred in as-cast samples. The matrix is supersaturated, intermetallics and centerline segregation are reduced. Electrical conductivity tests and BF images results prove the supersaturated matrix. There was also a slight decrease in the annealing temperatures required for recrystallization. Additionally, there was an approximately 30% increase in microhardness. Tensile and Erichsen results also confirm the strength increases.

1. INTRODUCTION

Aluminum's usage areas and consumption rate increase day by day as it has many unique properties. Specific strength, lightness, very good thermal and electrical conductivity and corrosion resistance make it very competitive [1] [2].

Aluminum flat products have been the choice of use in many different sectors for many years. Aluminum flat products are widely used in areas such as packaging, automotive, heating-cooling, architectural structures etc. One of the main reasons why it is preferred is that it can be easily shaped with a press. They are used as heat shields in the automotive industry, as food containers in the food industry, and as candle containers in decorative products.

Aluminum sheets can be produced by the twin roll casting method (Twin roll casting, TRC). Twin roll casting method (TRC) is based on the principle of solidification by absorbing heat from the interface formed by feeding the liquid metal between two water-cooled rolls through a ceramic tip. Then, it takes its final shape with or without annealing by cold rolling and slitting/cutting to length processes [3].

In the twin roll casting method, 2 main rolls and 2 roll shells mounted on them in a shrink fit are used. While the core part of the rollers is responsible for creating the structural integrity and stability of the system with its design features, the main function of the roller shell is to absorb the heat from the liquid metal entering between the roller gap and transfer it to the cooling medium circulating at the interface between the core and the shell. During thermal heat transfer, microcracks occur on the roller surfaces. The plate is subjected to turning and grinding processes in order to eliminate these cracks that affect the surface quality. When the roller diameter decreases to a critical value, it is replaced with a new shell and made usable again [4].

In the flat product manufacturing industry, alloy steel shells are widely used as roll shell material traditionally. To achieve the longest lifespan and the best conductivity, mechanical and thermal properties must be perfectly balanced. Here, there are two options to consider. Either a large rise in productivity statistics with optimum lifespan is desired, or traditional productivity figures with a significantly longer shell life are adhered. Due to its great thermal conductivity, copper is the primary option. But using pure copper will severely shorten its life because of its poor mechanical qualities. Therefore, alloying elements like cobalt and beryllium enhanced its

2.2. Method

In this study, one of the widespread usage area in flat rolled products commercial grade 5005 aluminum alloy sheets cast by the twin-roll casting method were produced in the 5-7 mm thickness range. Process 1, 2, 3 and 4 represent the routes of the samples casted with the St/St shell pair and process 5, 6, 7 and 8 casted with the St/Cu shell pair. After casting, it was cold rolled with a Delta brand laboratory scale rolling machine with a cold deformation rate of 82% from a casting thickness of 5-7 mm. After that, intermediate annealing was applied to the samples at different temperatures: 330, 350, 370 and 390. These routes are indicated in the flow chart given in Figure 2.

strength and service life [5].

Using an alloy copper shell is an alternative to the steel shell. The purpose of this study is to improve the production parameters by reducing centerline segregation, obtaining equiaxed and fine grain size as a result of rapid solidification, improving mechanical properties, and enabling the production of aluminum plate with the steel/copper shell pair combination [6].

This investigation looked at the electrical conductivity values, hardness profile through thickness, grain size, intermetallic particle size/distribution, and microstructural components for both surfaces subjected to various solidification pathways. Using a steel/steel shell pair, the outcomes were compared to those of conventional manufacture of 5005 aluminum alloy.

2. MATERIAL AND METHOD

In this study, the compositions of melting furnaces were set up considering EN 573-2 standards. This standard covers a code designation system applicable to aluminum and aluminum alloys as specified in the relevant standards. These are European Norm standards determined for the chemical composition and shape of formable products. As shell materials, beryllium alloy copper shells and alloy steel shells were used in Novelis PAE Jumbo 3CM® Continuous Caster Machines.

2.1. Material

As the main materials, two commercial grade 5005 aluminum alloy sheets with a thickness of 5-7 mm were used. One 5005 aluminum alloy plate was produced with an alloy steel/steel roller pair, and the other 5005 plate was produced with a beryllium alloy copper/alloy steel shell roller pair. As-cast samples produced with steel/steel and steel/copper shell are given in Figure 1.

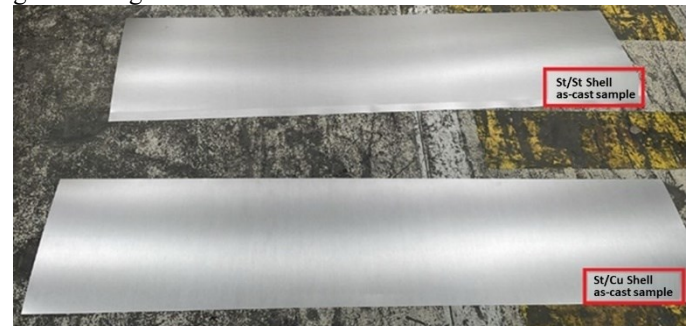


Figure 1. As-cast samples produced via steel/steel and steel/copper shell pair

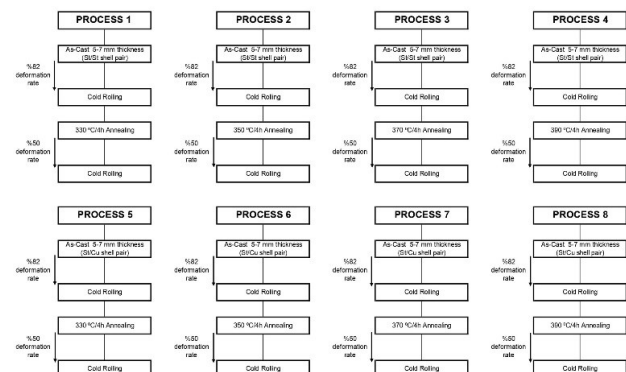


Figure 2. Route flow charts of the processes

In the first stage, it was cold rolled with a Delta brand laboratory scale rolling machine with a cold deformation rate of 82% from a casting thickness of 5-7 mm.

Then, 4 different samples were taken and an intermediate annealing process was applied for 4 hours at 4 different temperatures as 330, 350, 370 and 390 °C in processes 1, 2, 3, and 4 respectively. The intermediate annealing process was carried out in Nabertherm brand laboratory annealing furnaces. The samples, to which 4 different intermediate annealing recipes were applied, were reduced to their final thickness by cold rolling with a 50% cold deformation rate.

2.3. Analysis

The samples produced considering to EN 573-2 standard were subjected to elemental analysis using Thermo Scientific ARL 3460 optical emission spectrometer device. The result ranges of the spectrometer are given in Table 1.

Table 1. The result ranges of the spectrometer of samples considering to EN 573-2

Element	% weight
Si	0.85-0.95
Fe	0.27-0.35
Cu	0.002-0.010
Mn	0.015-0.020
Mg	0.55-0.75
Cr	0.001-0.005
Ni	-
Zn	0.002-0.010
Ti	0.02-0.03
Ga	-
V	0.01-0.03
Others	-
Al	98.95

The samples obtained as a result of the determined routes were prepared for metallographic examination under the with the ZEISS Scope.A1 optical microscope. The samples, cut to appropriate sizes and embedded in epoxy resin, were first grinding 500, 1200 and 2500 grit respectively and then subjected to final polishing with 3 µm SiC suspension. Electrolytic etching was done with tetrafluoroboric acid using the Struers Tegramin-30 device. Electrolytic etching was performed with HF on images taken in BF (bright field) mode. Microstructure images were obtained under polarized light and BF. Struers brand device was used for sample sanding and etching processes. Metallographic examinations were made with the ZEISS Scope.A1 optical microscope. In addition to the optical microscope, SEM (Scanning Electron Microscope) images were examined at 500X, 1000X and 2000X magnifications and EDS (Energy Dispersive Spectroscopy) field analyzes were performed with the ZEISS EVO MA 15 scanning electron microscope for detailed microstructural and elemental examinations of the samples.

In order to analyze the mechanical properties of the samples used in the processes, two-way tensile tests, 0° and 90°, were applied on the Zwick/Roell 50kN testing device considering to DIN EN ISO 6892-1 standards. In tensile tests, yield strength, tensile strength and % elongation values were obtained. In addition, the values were examined by applying Erichsen tests on the same device considering to ISO 20482 standards. Microhardness measurements were taken from the cross-

section of the samples in Vickers using the Future-tech Vickers microhardness measuring device. Measurements were recorded with parameters for 10 seconds under 10 gf load.

Electrical conductivity values of the samples taken during the processes were also obtained using the Fischer brand conductivity measuring device. Conductivity values were measured by setting the frequency to 480 kHz and allowing penetration to a depth of approximately 150 µm from the surface.

3. RESULTS AND DISCUSSION

3.1. Microstructural Analysis

In the study, microstructure images were obtained parallel or perpendicular to the casting or rolling direction. They are called as taking images in perpendicular (longitudinal-L) and parallel (transverse-T). It is shown in Figure 3.

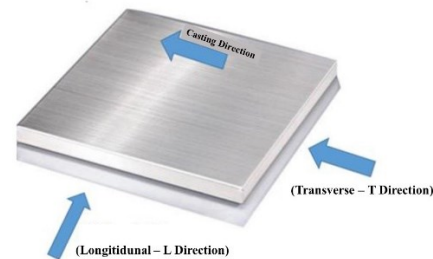


Figure 3. Sample preparation directions according to casting or rolling direction in microstructure imaging

3.1.1. Microstructures of As-Cast Samples

The microstructure images of the as-cast thickness samples are presented in Figure 4, 5, 6 and 7. In these as-cast microstructure images, Figure 4, 5 and 6 are polarized microstructure images. Additionally BF (bright field) images on the optical microscope were obtained for examining centerline segregation and amount of intermetallics. They were presented in Figure 7. Grain elongations specific to the twin-roll casting structure are present in both materials made with steel and steel shell and those cast with steel and copper shell. Polarized microstructure images in Figures 4 and 5 make grain elongations quite evident. The reason for these grain elongations is that rolling is a necessary step in the process, and the aluminum solidifies between the two rollers. Once more, upon closer inspection of these pictures, it is evident that the upper and lower portions in contact with the rollers have a finer-grained microstructure than that in the middle area due to their rapid solidification. It is evident that the microstructure is equiaxed and comparatively coarser grained toward the center. The grain structure on the surface in touch with the copper shell at the bottom of Figure 4(b) and 5(b) have been found to exhibit a coarser-grained and more equiaxed microstructure than the grain that on the surface in contact with the steel shell at the top. This structural difference resulted from partial dynamic recrystallization caused by the deformation effect and quicker solidification of the copper shell owing to its superior heat conductivity as compared to the alloy steel shell. This phenomenon, which is a result of precipitation of dispersoids from a highly supersaturated matrix, is known as the Zener Drag phenomenon [7]. Under an optical microscope, the structural variations of the materials cast with both shells on the

surfaces in contact with the rollers were examined under polarization, and the results are shown in Figure 6.

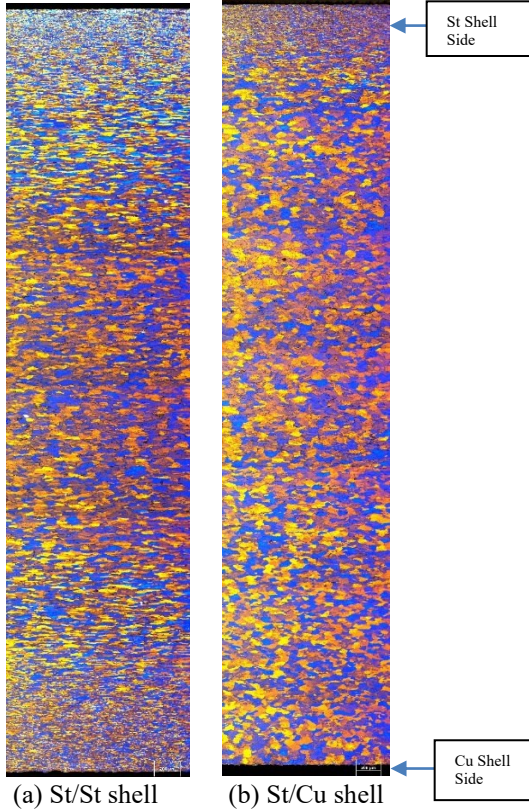


Figure 4. Polarized microstructure images of as-cast samples from T direction

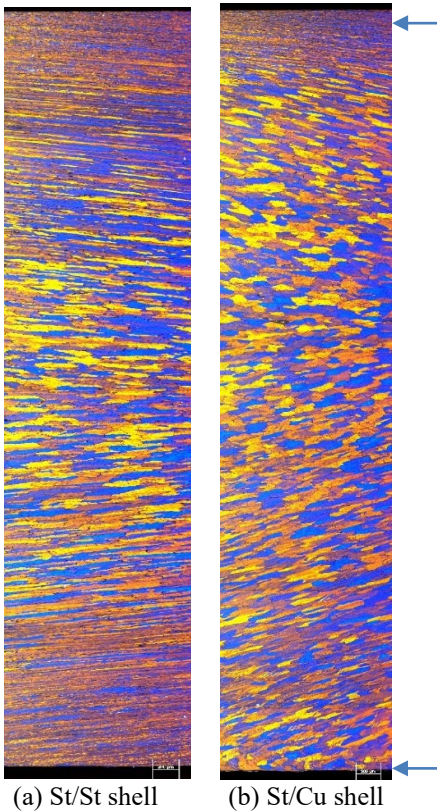
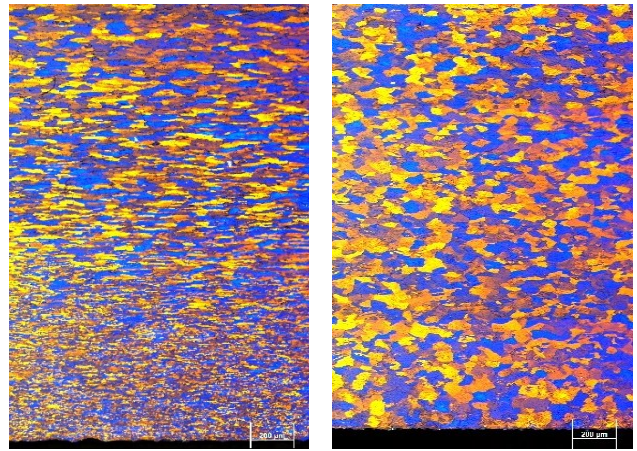


Figure 5. Polarized microstructure images of as-cast samples from L direction



(a) St shell (b) Cu shell

Figure 6. Polarized images of the surfaces of as-cast 5005 aluminum sheets in contact with different shells taken under an optical microscope

One of the main issues with the twin-roll casting process, centerline segregation, has considerably lessened when examining the BF images of the as-cast thickness samples obtained in the L direction in Figure 7. Furthermore, in the sample produced with steel/steel shell, the centerline segregation was in the center; however, in the sample produced with steel/copper shell, it was moved by 0.503 mm from the center to the steel shell side. By preventing intermetallics from precipitating and achieving a greater solidification rate in copper shell casting, a more supersaturated matrix is formed. Intermetallic precipitations or centerline segregation, were therefore moved towards the steel shell surface as a result of inhibiting the production of intermetallics on the copper side. In addition, when looking at the image in Figure 7(c), it is clearly seen that the intermetallics are abundant on the steel shell surface and in very small amounts on the copper shell surface.



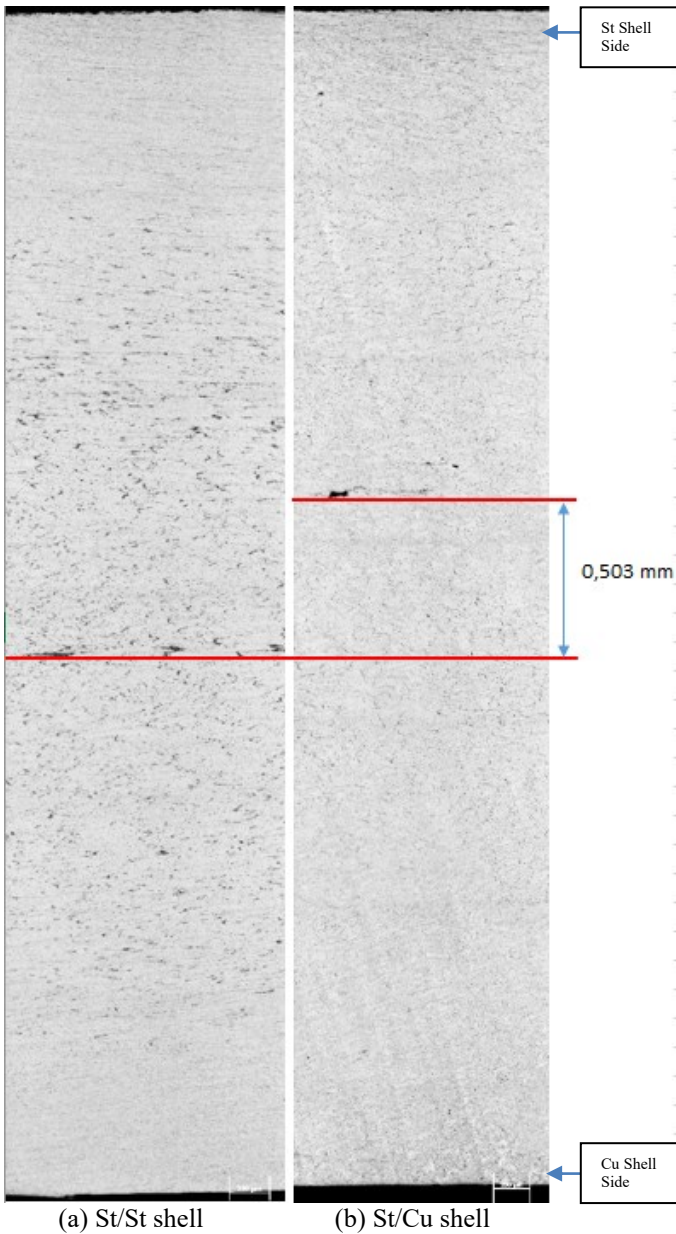


Figure 7. BF images of as-cast samples from L direction and motion distance of centerline segregation to St shell side
 To investigate centerline segregation in greater depth, SEM images and EDS area scan analyses were obtained. Figure 8 displays SEM images obtained at 500X, 1000X, and 2000X magnification.

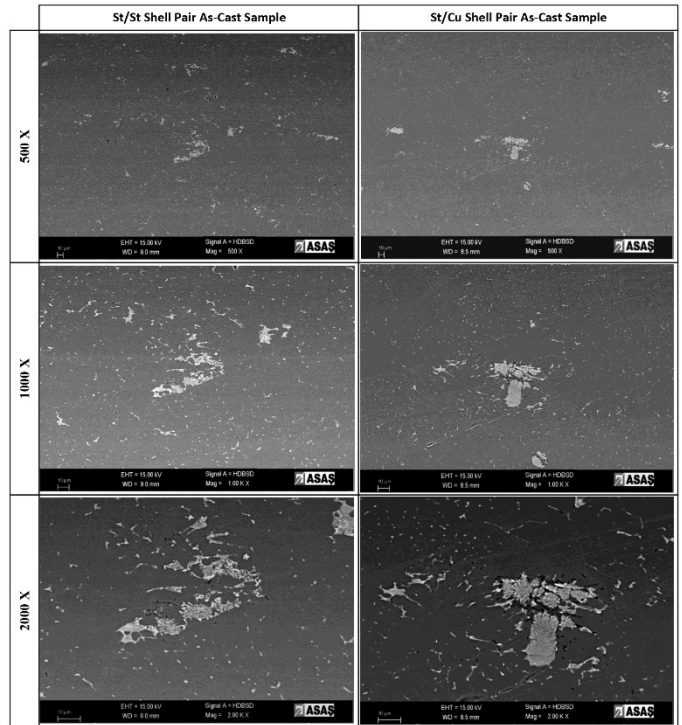


Figure 8. SEM images of as-cast samples magnified by 500X, 1000X, and 2000X

In the sample shown in Figure 9, produced with steel/steel shell pair, area scans were performed from the intermetallic and matrix and their graphs are given in Figure 10 and 11 and their results are given in Table 2.

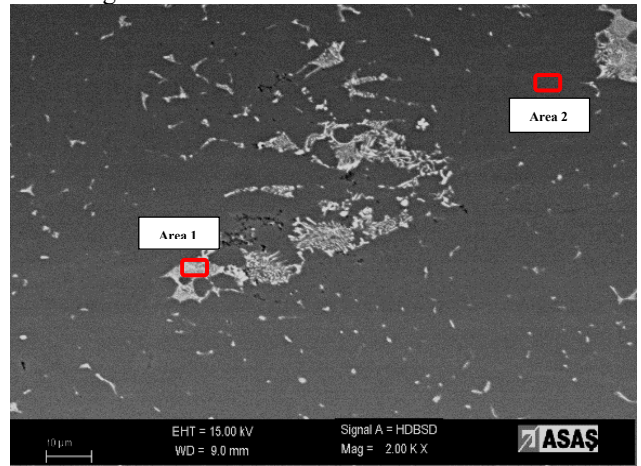


Figure 9. SEM image of centerline segregation obtained from as-cast sample produced with St/St shell.

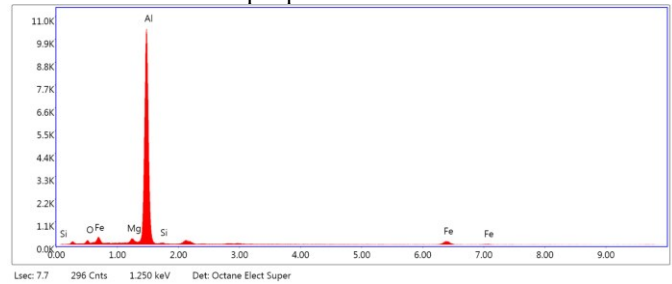


Figure 10. EDS graphs of field scan 1 (St/St shell)

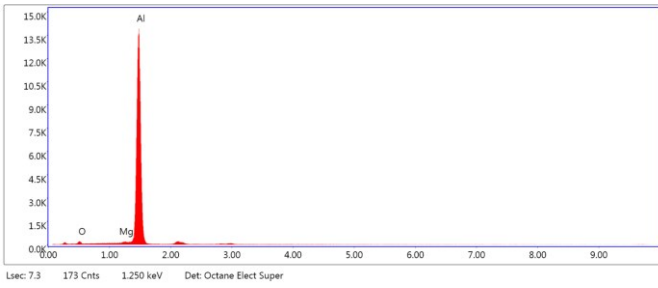


Figure 11. EDS graphs of field scan 2 (St/St shell)

Table 2. Elemental analysis of EDS area scanning 1&2 and their %weight ratios (St/St shell)

Element	Area 1	Area 2
O	1.75	1.76
Mg	2.20	1.24
Al	83.11	97.00
Si	1.14	-
Fe	11.81	-

For other sample produced with St/Cu shell pair, shown in Figure 12, area scans were performed from the intermetallic and matrix and their graphs are given in Figure 13 and 14 and their results are given in Table 3.

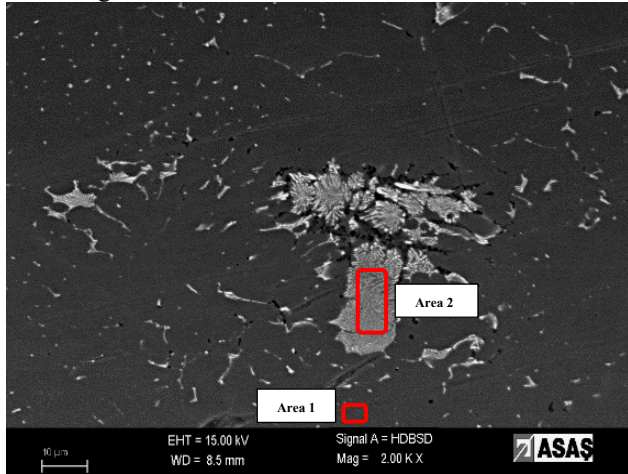


Figure 12. SEM image of centerline segregation obtained from as-cast sample produced with St/Cu shell.

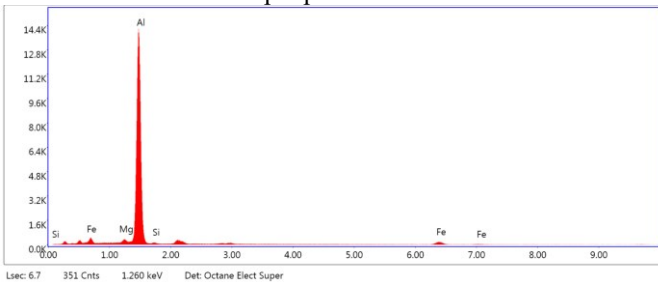


Figure 13. EDS graphs of field scan 1 (St/Cu shell)

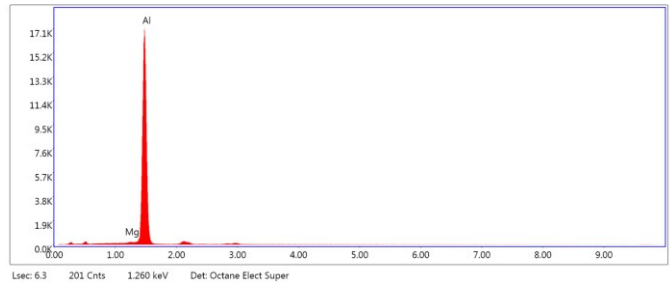


Figure 14. EDS graphs of field scan 2 (St/Cu shell)

Table 3. Elemental analysis of EDS area scanning 1&2 and their %weight ratios (St/Cu shell)

Element	Area 1	Area 2
O	-	-
Mg	1.76	1.07
Al	87.25	98.93
Si	1.19	-
Fe	9.80	-

In the SEM-EDS area scans performed from the as-cast samples in both the steel/steel and steel/copper shell pairs, area scans number 1 were performed from the intermetallics, while area scans number 2 were performed from the matrix. The content of predominantly Al and some Mg in the matrix material is characteristic of the 5005 aluminum alloy. Fe, Si and O, which appear in area scan 1, represent the composition percentages of intermetallics contained as centerline segregation in the material.

In the sample produced with the steel/steel shell pair, it was determined that while the iron content was 11.81%, at the steel/copper shell pair side, it decreased to 9.80% and the magnesium content decreased from 2.20 to 1.76. Again, while oxygen was present in both the matrix and the intermetallic in the steel/steel shell pair, the presence of oxygen was not found at the steel/copper shell pair side. It was determined that the silicon ratio remained the same in both samples.

3.1.2. Microstructures of Annealing Samples

The casting samples were reduced to an intermediate annealing thickness with being rolled at an 82% cold deformation rate. It was decided to anneal at four distinct intermediate temperatures: 330°C, 350°C, 370°C, 390°C and four hours annealed for each sample. Then, their polarized microstructure images were given in Figure 15.

The cold deformation rate is inversely proportional to the annealing temperature and time. The quantity of energy absorbed in the structure as a result of the rolling effect is crucial in the recrystallization annealing process. Low temperature will be adequate for the grains to recrystallize during annealing if a high percentage cold deformation rate is applied since there will be a large amount of energy retained in the structure [8].

Despite the high deformation rate, intermediate anneals at 330°C and 350°C for 4 hours each were insufficient for recrystallization due to heterogeneous grain structure between the surface and central regions, despite the presence of equiaxed grains in the central region. Intermediate annealing at 370°C for 4 hours results in recrystallization of grains at the surface and improved structural homogeneity and equiaxiality. Intermediate annealing at 390°C for 4 hours resulted in grain growth as tiny grains that recrystallized because of the high

temperature dissolved into the framework and diffused into bigger grains. This scenario is described by the Ostwald ripening process [9] [10].

All intermediate annealing temperatures resulted in grain size differences on the upper and lower surfaces contacting the rollers. Grain development on the outermost surfaces during intermediate annealing is a common occurrence using the TRC technique, regardless of alloy [10]. In Figure 15, the microstructure of the sample generated with Steel/Steel shell, which was intermediate annealed at 370°C for 4 hours, is identical to that of the sample produced with the steel/copper shell pair, which was intermediate annealed at 350°C for 4 hours. It has been hypothesized that since the grains actively recrystallize during casting due to the copper shell effect, the recovery and recrystallization phases are completed at lower temperatures during annealing.

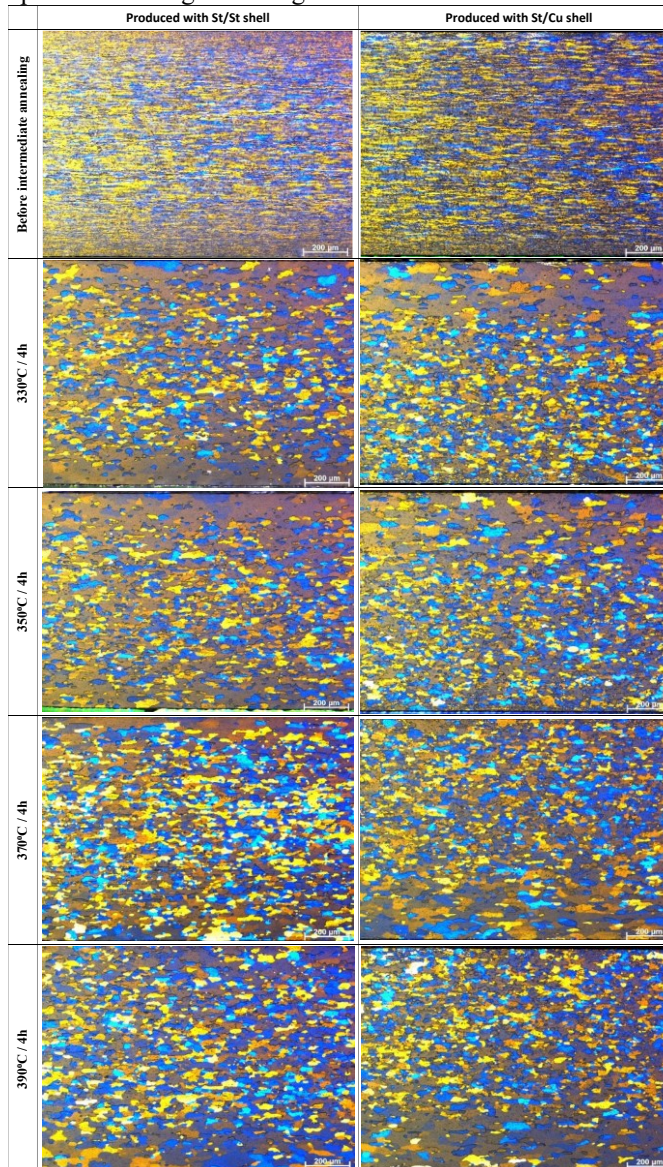


Figure 15. Polarized microstructure images of samples that different annealing temperatures produced with St/St and St/Cu shell pairs

3.2. Mechanical Properties Analysis

3.2.1. Tensile Strength Testing

Tensile tests were performed in each stage to evaluate mechanical properties. The test results are shown in Table 4.

Some changes occur in both the physical and mechanical properties of the cold-treated material. As a result of plastic deformation applied to the material, strength, hardness and electrical resistance increase. However, ductility decreases. In this case, the material becomes unable to continue plastic deformation. The reason for this is that the dislocation density, which is around 10^{10-12} m/mm³ when the shape starts, reaches 10^{16} m/mm³ after plastic deformation. Since each dislocation is a crystal defect, it produces lattice stresses within its environment, thus contributing significantly to the stored energy. Increasing lattice stresses are associated with an increase in the strain energy in the metal [11]. Annealing is applied in order to continue plastic deformation. During annealing, three events occur in the material microstructure, defined as recovery, recrystallization and grain growth, respectively. After annealing, hardness decreases, ductility increases and the material becomes re-formable. This situation is shown graphically in Figure 16 below [12].

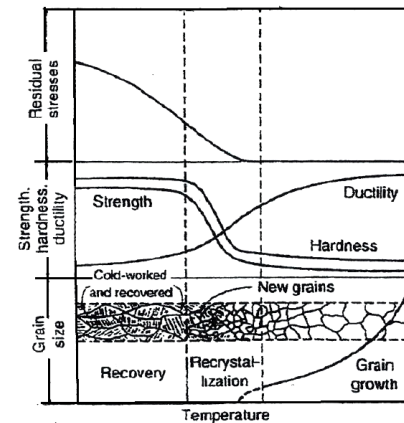


Figure 16. Effect of annealing temperature on hardness, strength and ductility [12]

In this study, tensile strength results of the samples cold rolled were showed that increased firstly compared as-cast sample. After the annealing, tensile results were decreased as it mentioned previous paragraph. In the tensile results of the cold-rolled pre-annealing samples, both as-cast thickness and 82% cold deformation rate, the yield and tensile strength values of the plates cast with copper/steel shell were higher than those of the plates cast with steel/steel shell. Rollers cooled with water exhibit better strength values due to the copper shell's higher thermal conductivity and thinner, equiaxed microstructure.

When the tensile tests performed on the samples taken after annealing of the sheets annealed at different temperatures were examined, no significant difference was seen in the strength values.

Table 4. Tensile strength test results for each phase

ROUTES	Direction of Sample ^a	Yield %0,2 MPa		Tensile MPa		Elongation (%)	
		St/St Shell	St/Cu Shell	St/St Shell	St/Cu Shell	St/St Shell	St/Cu Shell
As-Cast Sample	0°	103	127	133	148	13,5	6,4
	90°	107	129	135	156	10,9	11,6
The samples before annealing	0°	222	250	228	256	3,2	2,6
	90°	228	250	238	264	3,3	3,5
330°C / 4h annealed sample	0°	49	54	107	109	24,8	22,7
	90°	50	53	107	108	28,5	22,3
350°C / 4h annealed sample	0°	49	53	106	109	23	25,1
	90°	53	51	108	107	26,8	24,3
370°C / 4h annealed sample	0°	56	55	108	110	24,3	25,3
	90°	53	52	108	108	30,6	26,3
390°C / 4h annealed sample	0°	50	53	108	109	26,3	21,5
	90°	53	52	109	109	28	27,5
330°C / 4h annealed and after that % 50 cold rolled final thickness sample	0°	165	167	166	169	0,7	0,8
	90°	173	172	177	178	0,4	0,6
350°C / 4h annealed and after that % 50 cold rolled final thickness sample	0°	165	167	165	169	0,3	0,6
	90°	176	175	181	180	0,6	0,6
370°C / 4h annealed and after that % 50 cold rolled final thickness sample	0°	166	169	167	171	0,6	1,9
	90°	177	178	178	182	0,3	0,5
390°C / 4h annealed and after that % 50 cold rolled final thickness sample	0°	164	171	165	173	0,4	0,9
	90°	176	181	178	184	0,3	0,4

The tensile test results of plates lowered to the final thickness revealed a significant loss in strength values for samples manufactured with St/St shell pair at annealing temperatures above 350°C. After annealing St/Cu shell pair plates, the final thickness sample tensile test results increased in direct proportion to annealing temperature. On the St/St side, despite tensile strength values was increased in direct proportion to annealing temperature at 330, 350 and 370°C, there was a little bit decreasing tensile strength value at 390°C. It is observed that the sample generated with St/Cu shell pair, which contains more grain boundaries due to the thinner and equiaxed microstructure resulting from the casting structure, has higher formability capabilities because it recrystallizes more uniformly after annealing.

3.2.2. Erichsen Cupping Testing

The Erichsen cupping test is extensively used in the industry to determine the maximum deep shrinkage qualities of plates in terms of distance. The samples were prepared and loaded onto the Zwick/Roell device using the Erichsen cupping equipment. It is calculated as the depth proportional to the force produced when the samples burst during the test. It is stated in millimeters. The Erichsen test results for each step (1-8) are shown in Table 5 and their graphics in Figure 17 below.

When the Erichsen test results were examined, very close values were obtained. When sorted, it is seen as Process 2 < Process 1 = Process 4 < Process 3 = Process 8 < Process 5 = Process 7 < Process 6.

Table 5. Erichsen cupping test results (mm)

Route	Erichsen Result (mm)	
	St/St	St/Cu
330°C / 4h annealed final thickness sample	6.6	7
350°C / 4h annealed final thickness sample	6.4	7.2
370°C / 4h annealed final thickness sample	6.9	7
390°C / 4h annealed final thickness sample	6.6	6.9

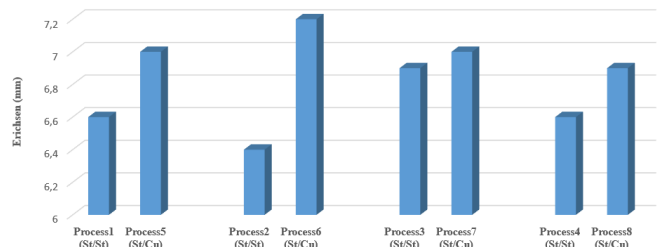


Figure 17. Comparative Erichsen cupping test results of St/St and St/Cu shells

According to the results, a dramatic decrease was observed in all samples annealed at 390°C and 4 hours compared to the other samples. This situation occurred as a result of grain growth as the annealing temperature was higher than that in other processes.

It was observed that Process 2 sample had the lowest Erichsen value. This is due to the fact that it is cast with the St/St shell pair and has a coarser grained microstructure compared to the St/Cu shell pair and cannot recrystallize sufficiently during annealing.

As a result of the processes applied to the samples produced with the St/St shell pair, the highest Erichsen value was taken from the Process 3 sample with 6.9 mm, which was annealed at 370°C and for 4 hours. It can be seen that the samples produced with the St/Cu shell pair were taken from the Process 6 sample, which was annealed at 350°C and 4 hours and obtained a result of 7.2 mm. The reason for this situation is that in the samples cast with steel/copper shell, copper has a higher heat conduction coefficient, partial dynamic recrystallization during casting and faster solidification, as well as dispersion hardening that occurs due to the saturation of the matrix with alloying elements.

3.2.3. Micro-hardness Testing

Microhardness tests were performed along the Vickers cross-sections (L direction) of the materials produced with St/St and St/Cu shell pairs. Test results are shown in Table 6 and Figure 18.

Table 6. Microhardness values according to shell types and surfaces

Shell Type		Hardness (HV)
St/St	St side (upper surface)	57.9
	St side (bottom surface)	56.2
St/Cu	St side (upper surface)	66.7
	Cu side (bottom surface)	71.0

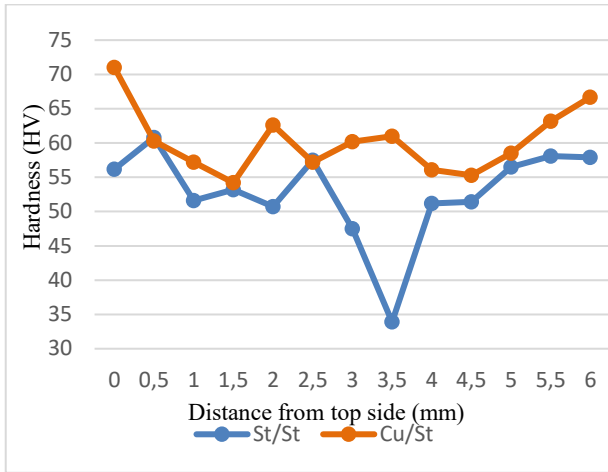


Figure 18. Microhardness measurement results from upper surface to bottom surface according to shell pair types

When the Vickers hardness tests performed were examined, while the hardness on the surface in contact with the copper shell was 71 HV, values of 57.9 - 66.7 HV were obtained on the surfaces in contact with the steel shell.

It is possible to obtain a supersaturated matrix with rapid solidification. Especially in the TRC method, centerline segregation, which is an important problem, is reduced by ensuring rapid solidification and a supersaturated matrix is obtained. A supersaturated matrix means that the major alloying elements are homogeneously dissolved in the matrix. With increasing matrix saturation, the lattice distortion caused by different atoms becomes more obvious. The density between secondary dendrite arms increases and prevents the movement and sliding of dislocations. For this reason, an increase in hardness occurs [13] [14].

A dramatic increase in hardness value has been achieved on the copper shell side compared to that in the steel shell. In addition, the samples produced with the St/Cu shell pair yielded higher hardness measurement results compared to the sample cast with the St/St shell pair.

3.3. Electrical Conductivity Analysis

Electrical conductivity tests were carried out for all samples. The results and graphs in MS/m units are given in Table 7 and Figure 19. In Table 7, "% Change" values are calculated as a percentage by dividing the difference between the first value and the last value by the first value. Also, this calculation describes in Equation 1.

$$\% \text{ Change} = \frac{[MS/m_{(St/St)}] - [MS/m_{(St/Cu)}]}{[MS/m_{(St/St)}} \times 100 \quad (1)$$

Table 7. Electrical conductivity results in MS/m at 480 kHz frequency

Route	Electrical Conductivity (MS/m)		
	St/St	St/Cu	% Change
As-cast	30.5	29.9	2%
Pre-annealing	29.5	29.2	1%
330°C / 4h after annealing	31.5	31.8	-1%
350°C / 4h after annealing	31.5	31.7	-0.6%

370°C / 4h after annealing	31.4	31.5	-0.3%
390°C / 4h after annealing	31.2	31.3	-0.3%
Final thickness (330°C/4h)	31.2	31.4	-0.6%
Final thickness (350°C/4h)	31.1	31.3	-0.6%
Final thickness (370°C/4h)	30.9	31.2	-1.0%
Final thickness (390°C/4h)	30.8	31	-0.6%

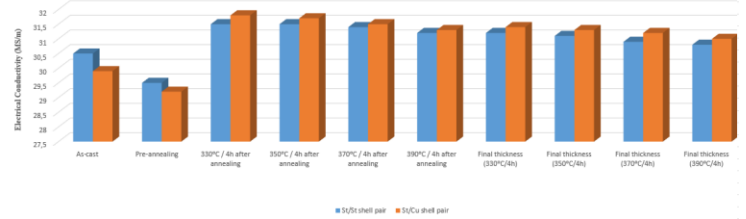


Figure 19. Comparative electrical conductivity test results of St/St and St/Cu shells

It is known that as matrix supersaturation increases, its electrical conductivity decreases inversely [15]. Considering Table 7, the minimum electrical conductivity value was obtained in the as-cast sample produced via the St/Cu shell pair. This low electrical conductivity result obtained on the copper shell side verified that the matrix is supersaturated. Additionally, when the electrical conductivity values of the as-cast and annealed samples are examined, it is seen that the samples produced with the St/Cu shell pair are annealed (31.5-31.8 MS/m) and as-cast (29.9 MS/m). This situation proves that the sample produced via St/Cu shell pair promises a higher potential for precipitation. According to the results obtained in all routes of the samples, produced with St/St and St/Cu shell, there were as-cast samples with the most significant change with a difference of 2%. It coincides with the result that the amount of the supersaturation in the as-cast sample using copper shell is high and the electrical conductivity value is minimum. No remarkable difference could be detected in other samples.

4. CONCLUSIONS

The results of this study were examined in terms of production parameters, microstructural, mechanical and electrical conductivity.

In production parameters, line speed and productivity increase by approximately % 40-60 when the St/Cu shell pair is used. With the line speed, the Cu shell used in the lower roller completes one full rotation around itself in a shorter time. Copper rollers, which have a high heat conduction rate, have a lower thermal cycle life compared to steel shells due to the rapid formation of microcracks. Roller pressures were applied lower because it has lower properties than steel in terms of mechanical strength.

When the microstructure results are examined, the Cu shell, which enables high heat transfer, provides supersaturation in the matrix by providing partial dynamic recrystallization along with some rolling force. And it has been proven that this method prevents both centerline segregation and intermetallic formation in general.

When the results of electrical conductivity tests were examined, remarkable results were obtained in both as-cast and annealed samples. The minimum electrical conductivity result in the as-cast state with a value of 29.7 MS/m confirmed the

existence of a supersaturated matrix. The difference in maximum conductivity existing between the annealed sample and the as-cast sample showed that it promises a higher chance for precipitation. Additionally, it has been shown that it also reduces the annealing temperature slightly, thanks to partial dynamic recrystallization during casting.

Mechanical properties coincide with microstructural investigations. There was approximately 30% increase in the hardness value on the surface in contact with the Cu shell. Tensile and Erichsen results clearly show that the strength increases in production with Cu shell.

ACKNOWLEDGEMENTS

The Authors would like to thank Mr. Samet SEVİNÇ and Mr. Ahmet BİCAT, team members of ASAŞ Aluminum R&D Laboratory, for their valuable help in sample preparation for metallographic investigations and taking images and reports in SEM.

REFERENCES

- [1] Kammer, C., "Aluminum and Aluminum Alloys", 161-197., Berlin, 2018.
- [2] Gülver, M., Meydanoglu, O., Işıksaçan, C., "Softening Behavior of Direct Chill and Twin-Roll Cast AA 3105 Alloy", In Light Metals, Springer International Publishing, Pages 1143-1147, 2019.
- [3] Engler, O., Schäfer, C., Brinkman, H.J., Brecht, J., Beiter, P., Nijhof, K., "Flexible rolling of aluminum alloy sheet—Process optimization and control of materials properties", J Mater Process Technol, Vol. 229, Pages 139-148, 2016.
- [4] Dündar, M., Beyhan, B., Birbaşar, O., Altuner, H.M., Işıksaçan, C., "Surface Crack Characterization of Twin Roll Caster Shells and Its Influence on As-Cast Strip Surface Quality", Light Metals, Vol. 2013, Pages 491-495, 2016.
- [5] Spathis, D., Clemente, A., Tsiros, J., Arvanitis, A., Wobker, H.G., "The use of copper shells by Twin Roll Strip Casters", TMS Light Metals, Mar. 2010.
- [6] Denizli, F., Birbaşar, O., Dündar, K., Özçetin, Y., Ulus, A., İnel, C., "Characterization of 8006 Aluminum Alloy Casted by TRC Technology with Steel–Steel and Copper–Copper Roll Pairs", In TMS Annual Meeting & Exhibition, Pages 1050-1053, 2023.
- [7] Recrystallization and Related Annealing Phenomena. Elsevier, 2004.
- [8] Birol, Y., "Recrystallization of a supersaturated Al–Mn alloy", Scr Mater, Vol. 59, Issue 6, Pages 611-614, 2008.
- [9] Lifshitz, I.M., Slyozov, V.V., "The kinetics of precipitation from supersaturated solid solutions", Journal of Physics and Chemistry of Solids, Vol. 19, Issue 1-2, Pages 35-50, 1961.
- [10] Ratke, L., Voorhees, P.W., "Growth and Coarsening", Berlin, Heidelberg: Springer Berlin Heidelberg, 2002.
- [11] Raougui, A., Yildiz, K., "Investigation of recrystallization kinetics of AA5005 sheets after rolling by thermal analysis", Master of Science Thesis, Sakarya University, Sakarya, 2021.
- [12] Iqra Zubair Awan, I.Z.A., "Recovery, Recrystallization, and Grain-Growth", Journal of the chemical society of pakistan, Vol 41, Issue 1, Pages 1-1, 2019.
- [13] Jo, Y.H., et al., "Effects of casting speed on microstructural and tensile properties of Al–Mg–Si alloy fabricated by horizontal and vertical twin-roll casting", Journal of Materials Research and Technology, Vol. 26, Pages 8010-8024, 2023.
- [14] Zhang, J., Yuan, H., Zhang, T., Fu, J., Xu, G., Li, Y., "A novel approach to improve the macro-segregation defect and mechanical properties of Al–Mg–Mn aluminum alloys during twin-roll continuous casting", Journal of Materials Research and Technology, Vol. 22, Pages 3170-3179, 2023.
- [15] Mohammadi, A., Enikeev, N.A., Murashkin, M.Yu., Arita, M., Edalati, K., "Developing age-hardenable Al-Zr alloy by ultra-severe plastic deformation: Significance of supersaturation, segregation and precipitation on hardening and electrical conductivity", Acta Mater, Vol. 203, Pages 116503, 2021.